THE SEDIMENTARY THICKNESS OF UGEP AND ITS ENVIRONS, INFERRED FROM ANALYSIS OF ITS MAGNETIC DATA

Supported by tetfund TERTIARY EDUCATION TRUST FUND

Faustinus Chukwunweike Anyadiegwu[1], Obinna Christian Dinneya[1], Bassey Mfon Aniefon[1], Boniface Ikechukwu Ijeh[4] and Daniel Enyinnaya Azunna[2]*

[1]Department of Physics, Michael Okpara University of Agriculture, Umudike, PMB 7267, Umuahia, Abia State, Nigeria

[2]Department of Physics, Clifford University, Owerrinta, PMB 8001, Aba, Abia State, Nigeria

*Corresponding author: azunnad@cliffordduni.edu.ng

Received: November 18, 2018 **Accepted:** May 21, 2019

Abstract: Aeromagnetic magnetic map over Ugep, sheet 314, located in the southern Benue Trough Nigeria was acquired, processed and interpreted, to determine the structural trend, depth to these magnetic anomalies, and to correlate these anomalies with mineral potential of the study area. The Total magnetic intensity map was reduced to magnetic equator, then the residual map was produced and these were further interpreted both qualitatively and quantitatively using the First to third vertical derivatives, the Horizontal derivatives, analytic signal and the source parameter imaging techniques. The results from analysis show the variation in depth observed with different wavelength which is an indication of source depths, the structural trends of the rock in the areas are in the ENE-WSW, NE-SW, and NW to SE respectively, and a lot of positive signals from several places in the analytical signal map which is an indication an intense igneous activity occurring as near surface intrusion or very shallow basement, further confirmed by the depth estimates from the source parameter imaging shows a ranges of values from -2200 metres to -83 meters and more than 80 percent of the total study area has depth values above -83 meters. The abundance of intrusive bodies in the study area renders this part of the southern Nigerian sedimentary basins unattractive for petroleum exploration. However, the area possesses high potential for large accumulation of base metal mineralization.

Keywords: Hydrocarbon potential, magnetic basement, sedimentary thickness, structural trends

Introduction

Aeromagnetic survey is a common type of geophysical survey carried out using a magnetometer aboard or towed behind an aircraft allowing much larger areas of the Earth's surface to be covered quickly. Aeromagnetic survey has played a major role in the delineation of both metallic and none metallic minerals (Gunn, 1993). Mapping of appropriate stratigraphic horizons and identification of suitable structures, such as faults, folds, intrusions etc. are important aspects of the interpretation of magnetic data. Knowledge of the forms of anomalous responses due to different source geometry is fundamental to the estimation of magnetic source boundaries. Diagnostic Structural and stratigraphic signatures for mineralization is important here, however, these signatures are not always diagnostic, so, many similar but un-mineralised zone may occur due to these reason. It becomes essential for the incorporation of magnetic method with other geophysical methods such as radiometric method, Since mineralization processes can also affect radioelement contents of rocks, radiometric data become other useful tools in identification of potential mineralization (Dickson, 1997) and also an important tool in the basement depth determination and thickness of sedimentary section especially in hydrocarbon prospects.

There are many airborne geophysical methods, such as gravity, radiometry, magnetic and electromagnetic. However, their operations are founded or based on the different physical principles, methodology and physical properties such as density, magnetic susceptibility, electrical conductivity, radioactive property of the Earth materials. These can in turn be employed for the provision of solutions for various geological problems and structural mapping of an area. What will determine the type of geophysical method to be used is a function of the physical and chemical properties of the rock type, and these properties vary from rocks to rock and also from place to place on the earth surface (Roy, 1966). Magnetic susceptibility is the physical property which defines the behaviour of rock or earth materials to magnetism.

Location and geology of the study area

The Ugep area located in the Southern (Lower) Benue Trough in the South-eastern part of Nigeria. It is bounded by Longitude 8^{o}00' to 8^{o}30' and Latitude 5^{o}30' to 6^{o}00' (Fig. 1).

Sedimentation in the Lower Benue Trough commenced with the marine Albian Asu River Group, although some pyroclastics of Aptian – Early Albian ages have been sparingly reported (Ojoh, 1992). The Asu River Group in the Lower Benue Trough comprises the shales, limestones and sandstone lenses of the Abakaliki Formation in the Abakaliki area and the Mfamosing Limestone in the Calabar Flank (Petters, 1982). The marine Cenomanian – Turonian Nkalagu Formation (black shales, limestones and siltsones) and the interfingering regressive sandstones of the Agala and Agbani Formations rest on the Asu River Group. Mid-Santonian deformation in the Benue Trough displaced the major depositional axis westward which led to the formation of the Anambra Basin. Post-deformational sedimentation in the lower Benue trough, therefore, constitutes the Anambra Basin. Sedimentation in the Anambra Basin thus commenced with the Campanian-Maastrichtian marine and paralic shales of the Enugu and Nkporo Formations, overlain by the coal measures of the Mamu Formation (Fig. 2).

The Nsukka Formation and the Imo Shale mark the onset of another transgression in the Anambra Basin during the Paleocene. The shales contain significant amount of organic matter and may be a potential source for the hydrocarbons in the northern part of the Niger Delta (Reijers and Nwajide, 1998). In the Anambra Basin, they are only locally expected to reach maturity levels for hydrocarbon expulsion. The Eocene Nanka Sands mark the return to regressive conditions (Fig. 3).

The Nanka Formation offers an excellent opportunity to study tidal deposits. Well-exposed, strongly assymetrical sandwaves suggest the predominance of flood-tidal currents over weak ebbreverse currents. The presence of the latter are only suggested by the bundling of lamine separated from each other by mud drapes reflecting neap tides. A good outcrop of the Nanka Formation is the Umunya section, 18 km from the Niger Bridge at Onitsha on the Enugu – Onitsha Expressway (Obaje, 2009).

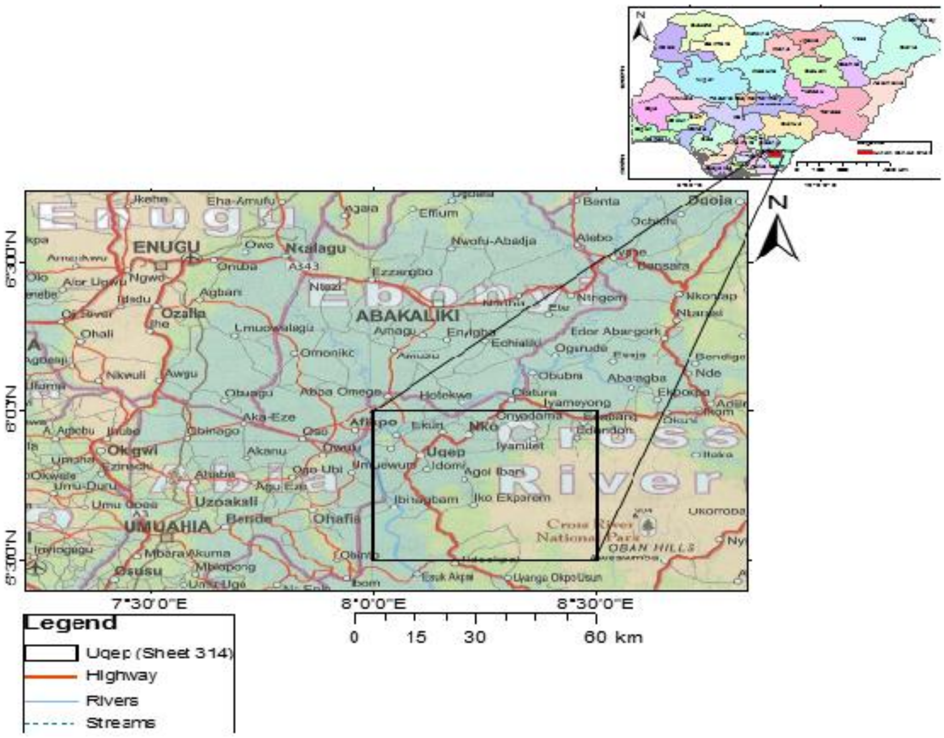

Fig. 1: The location map of the study area (Ugep sheet 314) in Cross River state

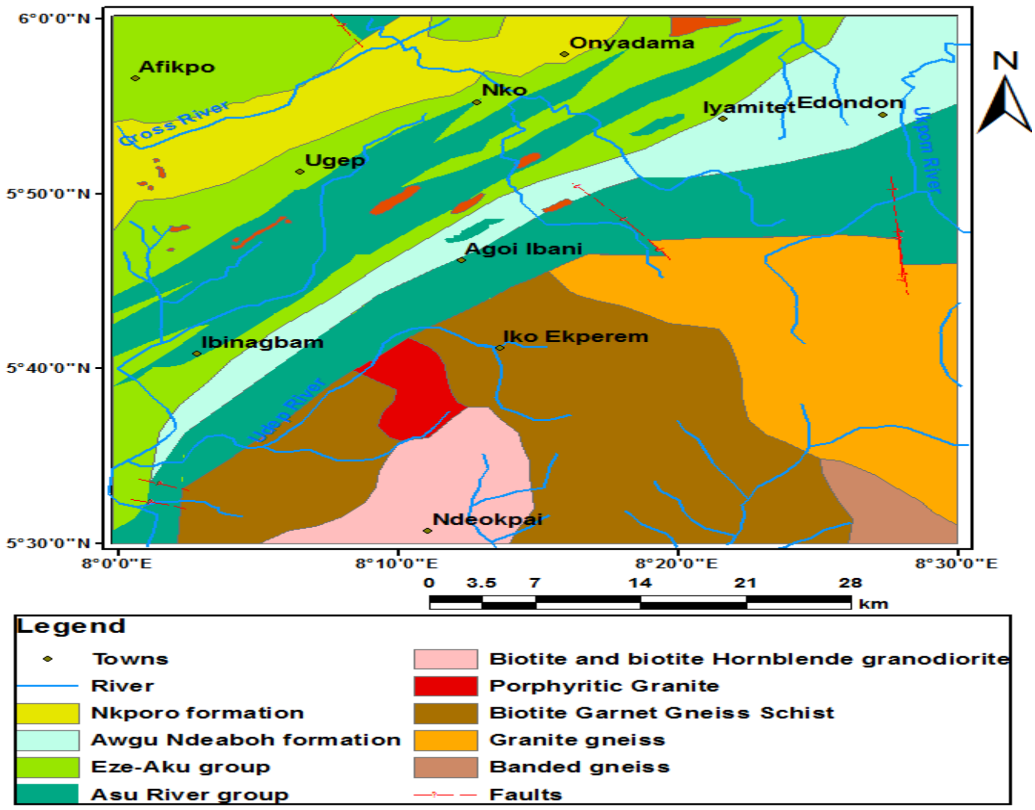

Fig. 2: The geologic map of Ugep area in the southern Benue trough (Modified after NGSA, 2010)

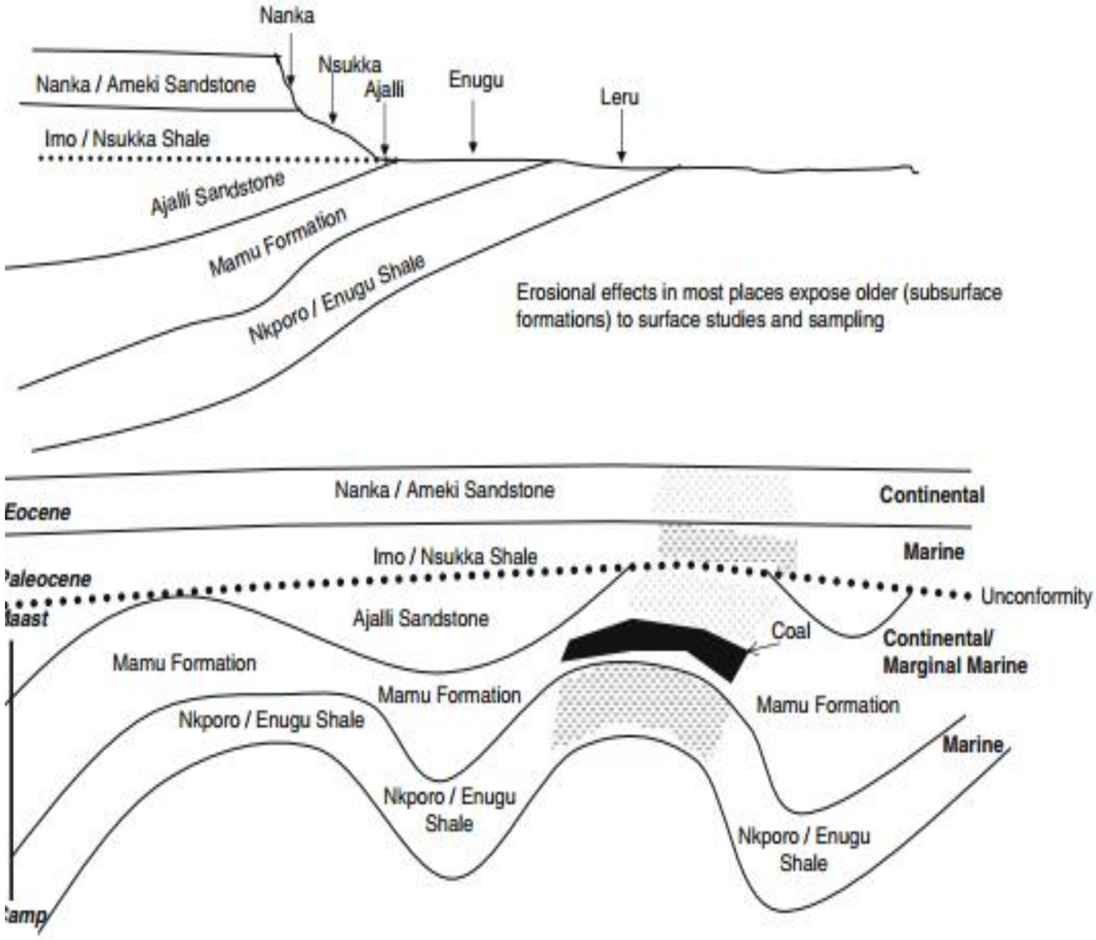

Fig. 3: Stratigraphic sucessions in the Anambra Basin (Obaje, 2009)

Exploitable economic deposits within the Anambra Basin – Calabar Flank include (i) Metalliferous minerals (iron ore and sulphides of copper, lead and zinc), (ii) Fossil fuels (coal, lignite, oil and natural gas), (iii) Industrial minerals (stone aggregates, clay, and limestone) and (iv) Chemical minerals (evaporates dissolved in salt springs) (Odebode, 2010).

Materials and Methods

Data acquisition

The aeromagnetic data was obtained from Nigerian Geological Survey Agency (NGSA). The Total Magnetic field Intensity (TMI) data was acquired and processed by Fugro survey Ltd. 3 Scintrex Cesium vapour magnetometers mounted in about 7 Cessna Caravan fixed-wing aircrafts at a time were used in acquiring the data. This arrangement coupled with seasonal variations required innovative approach in survey planning, instrument calibration, data compilation and grid merging. Projection method used in processing the data is the Universal Transverse Mercator (UTM) and the WGS 84 as Datum. Flight line direction was NW-SE. Tie lines were flown in the NE-SW direction. The surveys were flown at 500 m line spacing and 80 m mean terrain clearance generating a total of about 2 million line-km data (Reford *et al.*, 2012).

Data processing

The aeromagnetic data was processed using Oasis Montaj software, ARC GIS, and Surfer 15. Several linear transformations were performed to enhance features of interest, define structural trends and to estimate the thickness of the sediments. These transformation processes are well defined and the resultant maps follow.

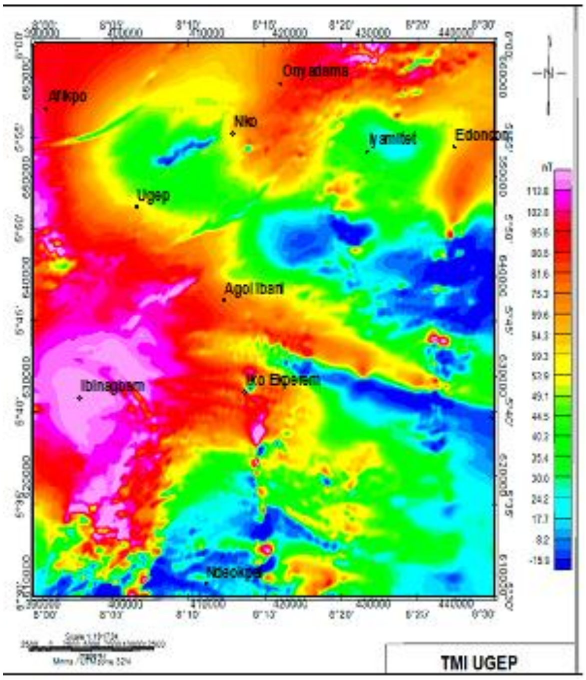

Fig. 4: The total magnetic intensity map of the study area

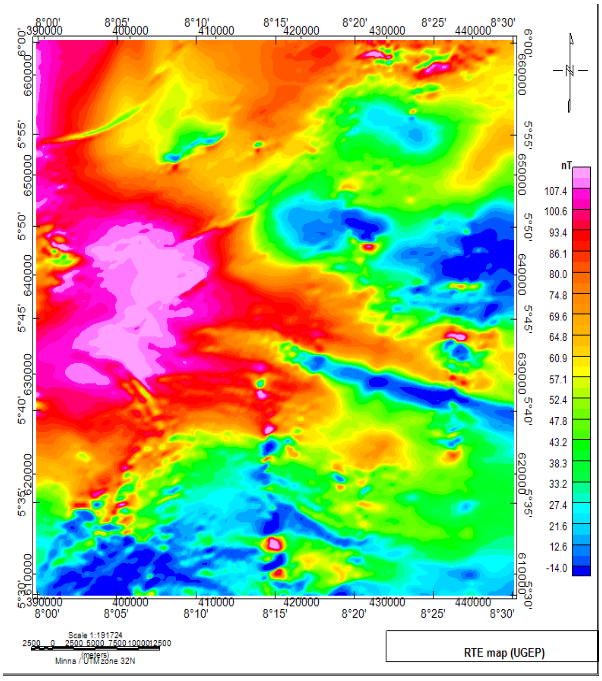

Fig. 5: The total magnetic intensity map reduced to magnetic equator

Reduction to the magnetic equator

Magnetic anomaly caused by a geological body or geological structure has an added complexity because of the core field. It depends not only on the physical properties of the sources, but also on the strength and direction of current geomagnetic field, even without considering remanent magnetization. Magnetic anomaly interpretation is mostly based on the theory of vertical magnetization, such as the tangent technique for calculating burial depths of magnetic plates or the inversion for magnetic interface. The interpretation becomes more complex at low latitudes due to the influence of dip magnetization, especially at the equator. Reduction to pole (RTP) is an important processing for aeromagnetic surveys, and it is the basis of magnetic anomaly interpretation. RTP takes convolution in space domain to reduce the effect of dip magnetization. Fourier Transform (FFT) made RTP more practicable, and RTP in the wave number domain has become an important transform method for potential fields. RTP at low latitudes, routinely computed in Fourier domain, is notoriously unstable. RTP filter is an enlargement type filter, and the noise is seriously enlarged which completely confuse the anomaly near the geomagnetic equator. Geophysicists have developed different solutions to overcome the difficulty of the reduction to the pole at low latitudes (Baranov 1957; Baranov and Naudy, 1964)

Technological advancements later gave rise to the classical method referred to as Reduction to equator (RTE). This method combines the phase reversal interpretation method for anomalies at low latitude to overcome the instability of RTP operation at the geomagnetic equator. The method can realize the stable reduction to pole in condition of the horizontal magnetization at or near the geomagnetic equator (Mendonca and Silva, 1993). The reduction to equator technique calculates TMI data as if the inducing magnetic field had a 0º inclination. For the purpose of this study, the reduction to equator technique was applied because the study area is close to the equator. The map resulting from this process is shown in Fig. 5.

Upward continuation

This technique is employed in magnetic interpretation to determine the form of regional gravity variation over a survey area, since the regional field is assumed to originate from relatively deep-seated structures. The high-wave number components of the observed field will be effectively removed by the continuation process. The upward continued field must result from relatively deep structures and consequently represents a valid regional field for the area. Upward continuation is also useful in the interpretation of magnetic anomaly fields over areas containing many near-surface magnetic sources such as dykes and other intrusions.

Upward continuation attenuates the high wave number anomalies associated with such features and enhances, relatively, the anomalies of the deep seated sources (Telford, 1990). The regional gradient (trend) can also be determined when upward continuation is done to a greater depth as shown in Fig. 6 and the regional anomaly trend of the study area can be determined.

Vertical derivatives

Computation of the first vertical derivative in an aeromagnetic survey is equivalent to observing the vertical gradient directly with a magnetic gradiometer and has the same advantages, namely enhancing shallow sources, suppressing deeper ones, and giving a better resolution of closely-spaced sources. Third and higher order vertical derivatives may also be computed to pursue this effect further, but usually the noise in the data becomes more prominent than the signal at above the second vertical derivative, thus, the First Vertical Derivative (1VD) and second vertical Derivative (2VD) transforms are the only transforms of this type that are routinely generated. The equation of the wave number domain filter to produce nth derivative is:

$$F(\omega) = \omega n \qquad (1)$$

The primary property of the second vertical derivative transform is that the Zero Contour represents the point of inflexion on the original anomaly curve which approximates the locations of edges of the causative bodies, providing that the bodies are shallow and have vertical sides. The first vertical derivative can be used as an alternative to a residual display (Andreasen and Zietz, 1969).

Horizontal gradient method

Magnetic data can be transformed to pseudogravity data using Fourier techniques (Hildenbrand, 1983) so that they behave like gravity data; thus the horizontal gradient of pseudogravity also has maximum magnitude directly over the boundary. The method normally is applied to gridded data rather than to profiles. The horizontal-gradient magnitude is contoured and lines are drawn or calculated (Blakely and Simpson, 1986) along the contour ridges. These lines presumably mark the top edges of magnetic or density boundaries. However, horizontal-gradient magnitude maxima (gradient maxima) can be offset from a position directly over the boundary for several reasons. Offsets occur when boundaries are not near-vertical, or when several boundaries are close together. This note predicts these offsets. Many other factors also cause offsets, but they are less straightforward and usually are only significant in local studies.

The gradient window method was developed to eliminate the filtering process required when regional and local gradients are superposed. Instead, the method is applied directly to unfiltered data and uses varying window size to focus on different scales of gradients.

Method

If F(x,y) I the magnetic field and $\frac{dF}{dx}$ ***and*** $\frac{dF}{dy}$ are derivatives in the -x and -y directions, then the HGM of the field F is define as;

$$HGM = \sqrt{\left(\frac{\partial F}{\partial x}\right)^2 + \left(\frac{\partial F}{\partial y}\right)^2} \quad (2)$$

Where x and y represent the orthogonal coordinate system of the gridded data and the HGM is computed at each grid point. The local maxima in the resulting HGM grid commonly form ridges that can be used to trace physical property boundaries (Blakely and Simpson, 1986).

The function peaks over contact with vertical regional magnetic field, vertical contact band strong magnetic source.

The gradient window method is a modification of the horizontal-gradient method that uses the HGM of the best fit plane in a moving window across a grid for regional gradients and the HGM of the residual for local gradients. The method gives results similar to the horizontal-gradient method applied to filtered data, but it eliminates the need for prior filtering that may be time-consuming and require a large data area in order to properly separate the regional field. A range of scales of regional gradients can be easily examined by changing the window size. A disadvantage is that the results only extend to within a half-window distance of the grid borders.

Analytical signal

Analytical signal of TMI has much lower sensitivity to the inclination of the geomagnetic field than the original TMI data, and provides a means to analyse low latitude magnetic fields without the concerns of the RTP operator. Analytical signal is a popular gradient enhancement, which is related to magnetic fields by the derivatives. Roest *et al*. (1992) showed that the amplitude of the analytic signal can be derived from from the three orthogonal gradient of the total magnetic field using the expression:

$$|A(x,y)| = \sqrt{\left[\left(\frac{dT}{dx}\right)^2 + \left(\frac{dT}{dy}\right)^2 + \left(\frac{dT}{dz}\right)^2\right]} \quad (3)$$

Where A(x,y) is the amplitude of the analytical signal at (x,y) and m is the observed magnetic anomaly at (x,y).

While this function is not a measurable parameter, it is extremely interesting in the context of interpretation, as it is completely independent of the direction of magnetisation and the direction of the Earth's field (Milligan & Gunn, 1997). This means that all bodies with the same geometry have the same analytic signal. Analytic signal maps and images are useful as they are not subject to the instability that occurs in transformations of magnetic fields from low magnetic latitudes. They also define source positions regardless of any remnant magnetization in the sources (Milligan & Gunn, 1997).

Source parameter imaging (SPI)

The SPI method (Thurston and Smith, 1997) estimates the depth from the local wave number of the analytical signal. The analytical signal (x, z) is defined by Nabighian (1972) as:

$$A_1(x,z) = \frac{\partial M(x,z)}{\partial x} - j\frac{\partial m(x,z)}{\partial z} \quad (4)$$

Where m(x,y) is the magnitude of the anomalous total magnetic field, j is the imaginary number, z and x are Cartesian coordinates for the vertical direction and the horizontal direction respectively. From the work of Nabighian (1972), he shows that the horizontal and vertical derivatives comprising the real and imaginary parts of the 2D analytical signal are related as follows:

$$\frac{\partial M(x,z)}{\partial x} \Leftrightarrow -\frac{\partial M(x,z)}{\partial z} \quad (5)$$

Where⇔ denotes a Hilbert transformation pair. The local wave number is defined by

Thurston and Smith (1997) to be to be

$$K_1 = \frac{\partial}{\partial x}\tan^{-1}\left|\frac{\partial M}{\partial z}\Big/\frac{\partial M}{\partial x}\right| \quad (6)$$

The concept of an analytic signal comprising second-order derivatives of the total field, if used in a manner similar to that used by Hsu *et al.* (1996), the Hilbert transform and the vertical-derivative operators are linear, so the vertical derivative will give the Hilbert transform pair,

$$\frac{\partial^2 M(x,z)}{\partial z \partial x} \Leftrightarrow -\frac{\partial^2 M(x,z)}{\partial^2 z} \quad (7)$$

Thus the analytic signal could be defined based on second-order derivatives,(x,z) where

$$A_2(x,z) = \frac{\partial^2 M(x,z)}{\partial x \partial z} - j\frac{\partial^2 m(x,z)}{\partial^2 z} \quad (8)$$

This gives rise to a second-order local wave numberK_2, where

$$K_2 = \frac{\partial}{\partial x}\tan^{-1}\left|\frac{\partial^2 M}{\partial^2 z}\Big/\frac{\partial^2 M}{\partial^2 x}\right| \quad (9)$$

The first- and second-order local wave numbers are used to determine the most appropriate model and depth estimate independent of any assumptions about a model. Nabighian (1972) gives the expression for the vertical and horizontal gradient of a sloping contact model as:

$$\frac{\partial M}{\partial x} = 2KFc\sin d\,\frac{h_c\cos(2I-d-90)+x\sin(2I-d-90)}{h_c^2+x^2} \quad (10)$$

$$\frac{\partial M}{\partial z} = 2KFc\sin d\,\frac{x\cos(2I-d-90)+h_c\sin(2I-d-90)}{h_c^2+x^2} \quad (11)$$

where K is the susceptibility contrast at the contact, F is the magnitude of the earth's magnetic field (the inducing field), c = 1 - $\cos^2 i \sin^2 \alpha$, α is the angle between the positive x-axis and magnetic north, *i* is the ambient-field inclination, tan I = $\sin i$/cosα, d is the dip (measured from the positive x-axis), $h_c$is the depth to the top of the contact and all trigonometric arguments are in degrees. The coordinate system has been defined such that the origin of the profile line (x = 0) is directly over the edge.

The expression for the magnetic-field anomaly due to a dipping thin sheet is;

$$M(x,z) = 2KFcw\frac{h_1\cos(2I-d)+x\sin(2I-d)}{h_c^2+x^2} \quad (12)$$

Reford (1964), where w is the thickness and *h1* the depth to the top of the thin sheet. The expression for the magnetic-field anomaly due to a long horizontal cylinder is;

$$M(x,z) = 2KFS\frac{\sin i}{\sin I}\frac{(h_h^2-x^2)\cos(2I-180)+2xh_h\sin(2I-180)}{(h_c^2+x^2)^2} \quad (13)$$

Murthy and Mishra is the cross-sectional area and *h*' is the depth to the centre of the horizontal cylinder. Substituting (10), (11), (12) and (13) into the expression for the first- and second-order (i.e. (6) and (9), respectively) local wave numbers, we obtain, after some simplification, a remarkable result as:

$$K_1 = \frac{(n_k+1)h_k}{h_k^2+x^2} \quad (14)$$

$$K_2 = \frac{(n_k+2)h_k}{h_k^2+x^2} \quad (15)$$

Where n_k is the SPI structural index (subscript k = c, t or h), and n_c= 0, n_t = 1 and n_h = 2 for the contact, thin sheet and horizontal cylinder models, respectively. From (14) and (15) above, it is evident that the first- and second-order local wave numbers are independent of the susceptibility contrast, the dip of the source and the inclination, declination, and the strength of the earth's magnetic field. The contact, thin sheet and horizontal cylinder are all two-dimensional models (infinite strike extent), so it is an implicit assumption of the SPI method that the geology is two dimensional. If the body is two-dimensional and there is no interference from nearby bodies, the depth estimate will be reasonable and the structural index should be constant over the entire area for which the response is anomalous.

Results and Discussion

Qualitative interpretation

Qualitative interpretation involves the identification of characteristic patterns and shape of anomalies with respect to particular geologic structure is one of the first steps in qualitative interpretation of a magnetic map. With the introduction of HRAM surveys, many near-surface geologic features are so clearly expressed that their geologic origin is obvious in color shaded-relief maps. In the shaded-relief (Gunn, 1997; Davies *et al*., 2004; Gay, 2004), folds look like folds, fault expressions can exhibit an echelon and anastomosing behavior (Langenheim *et al*., 2004) and individual dikes within swarms are clearly resolved (Modisi *et al*., 2000).

RTE (inverse)

The TMI of the study area was reduced to the Equator and then was further inversed to be able to produce a direct relationship between the observed intensity and the Magnetism, the RTE inverse map is displayed in Fig. 6 showing variation in magnetic intensities/susceptibility in different areas of the map, the inversed RTE ranges in intensity from -113.5 to values greater than -3.8.

Residual map

The Residual map of the area displayed in Fig. 7 which was produced by the regional-residual separation, it displays the residual field of the study area which is also described as a localized anomaly within the region. The first order residual map of the area has a variation in magnetic susceptibility/intensity which are depicted in pink (high magnetic intensity/susceptibility) and blue (low magnetic intensity/susceptibility), these variation can be observed in the residual map of the study area, the intensity values ranges from -37.1 to 39.4 nT, these anomaly also shows variation in wavelength which is an indication of the source of occurrence weather they are deep in origin or shallow in origin, long wavelength anomaly are of deep origin and short wavelength anomaly are from shallow origin which might be from a near surface intrusion or may occur as outcrops and are seen in the southern part of the Iko-Ekperem. The occurrence of this short wavelength (high magnetic susceptibility/intensity) anomaly are prominent in the Southern (Ndeokpai area), South-Eastern, Eastern, South-Western and some in the Northeastern (Iyamitet area) part of the study area respectively, and areas between the southern part of Ugep and the Northern part of Ibinagbam shows the occurrence of a low magnetic susceptibility anomaly and long wavelength indicates that the source as deep.

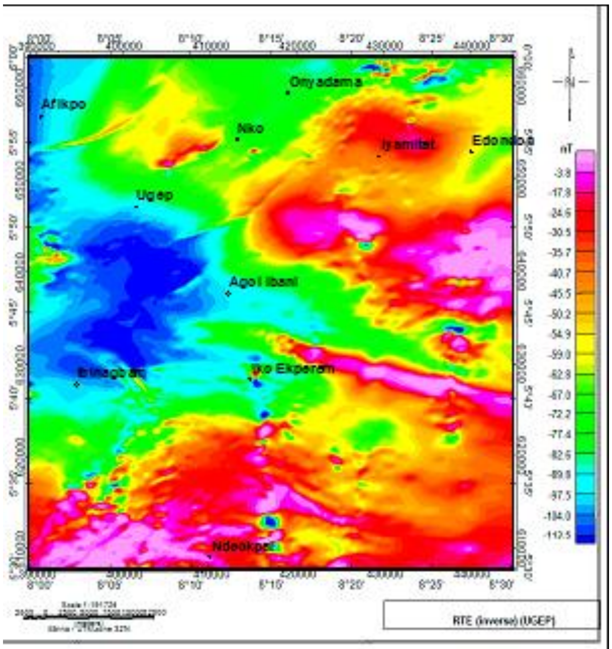

Fig. 6: The Total magnetic field intensity map (TMI) of the study area reduced to magnetic equator and then inversed

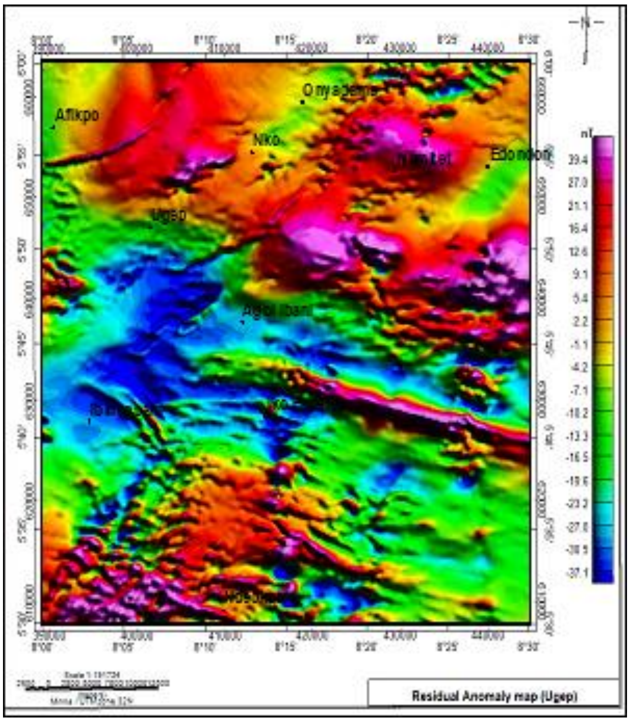

Fig. 7: The first order residual map of the study area

Vertical and horizontal derivatives

The Vertical derivatives emphasizes shallower anomalies and can be calculated either in the space or frequency domains. These operators also amplify high-frequency noise, and special tapering of the frequency response is usually applied to control this problem.

The first vertical derivatives (1vd) map of the study area (Fig. 8) shows the shallow anomaly sources within the area, these shallow anomaly magnetic sources could be as a result of near surface intrusions or as a result of the basement being depth being shallow, the first vertical derivatives is a type of an edge detection method which maps the edge of these bodies and also emphasizes the structures within the rocks, from the first vertical derivatives map we can see a variation in the trends of different magnetic bodies, and the structural orientations of the rocks in the study area and the structural trends of the basement in the area from a shallow magnetic source within the area.

The second vertical derivatives (2vd) (Fig. 9) further enhance structures nearer to the surface than the first vertical derivatives map and the third vertical derivatives (3vd) (Fig. 10) map of the study area also shows lineament and structures closer to the surface than the second vertical derivatives map, the lineament/ structures of the area were extracted from the second vertical derivatives map (Fig. 11) and the trend of these structures were plotted on the rose diagram to determine the trend in the area as seen in Fig. 12.

The main structural trend in the study area is said in the ENE-WSW directions, followed by the trend in the NE-SW and the lowest frequency in the NW-SE directions, these is consistent with the results gotten bay Oha *et al.* (2016), which described the orientation of the lineament in the lower Benue basin as running in the NE-SW direction and the results from the analaysis of the Ugep sheet 314 has a slight deviation to what was gotten from what gotten from the Landsat image processing and trend analysis done by Ezepue (1984); Oden (2012); Oha (2014) with a N–S and NW–SE subordinate trends reported in the area, however the ENE-WSW gotten from the results of our analysis must have been from been from a source at a depth below the surface.

Horizontal gradient map can be used to map the boundary of the various rocks with considerable magnetic susceptibility, and it can be used to differentiate different body of rocks, the Horizontal gradient map of the study area shows a lot of positive signals at different points on the study areas these can be taken as individual or separate rock types with magnetic signatures, the most prominent of such signatures are mostly Observed at the southern part of the Ugep sheet 314 around Ndeokpai and towards the Southwestern part of the area at the south of Ibinagbam area, and the signatures can also be observed at other areas around the East and in some other areas around the study area. These signals are boundaries of various lithology especially those of the basement within the area and these is an indication of the basement being very close to the surface or might even occur as outcrops in the area if correlated with the geological map of the area, these is what account for the clear signals observed in the Horizontal gradient map, they also show the structural trend of the rock in the study area. The Horizontal gradient map of the study area is displayed in Fig. 13.

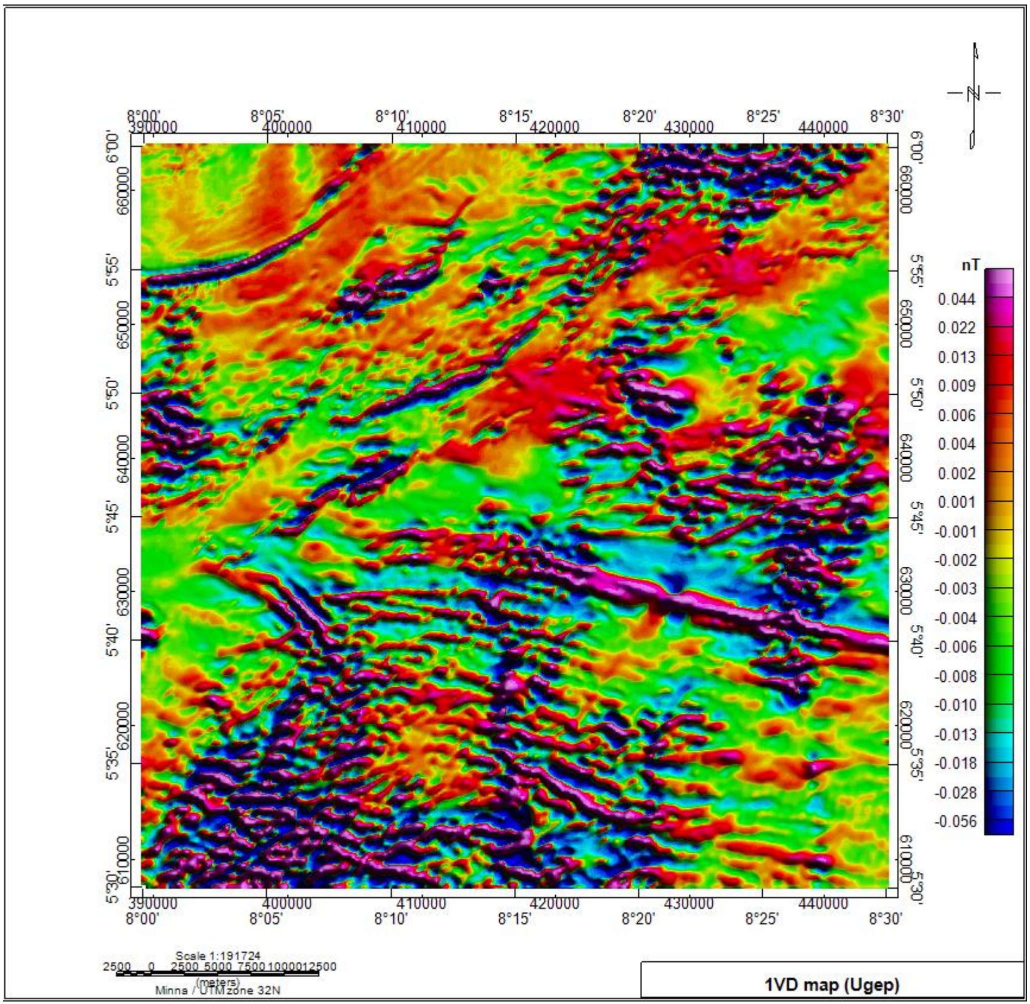

Fig. 8: First vertical derivatives map of the study area

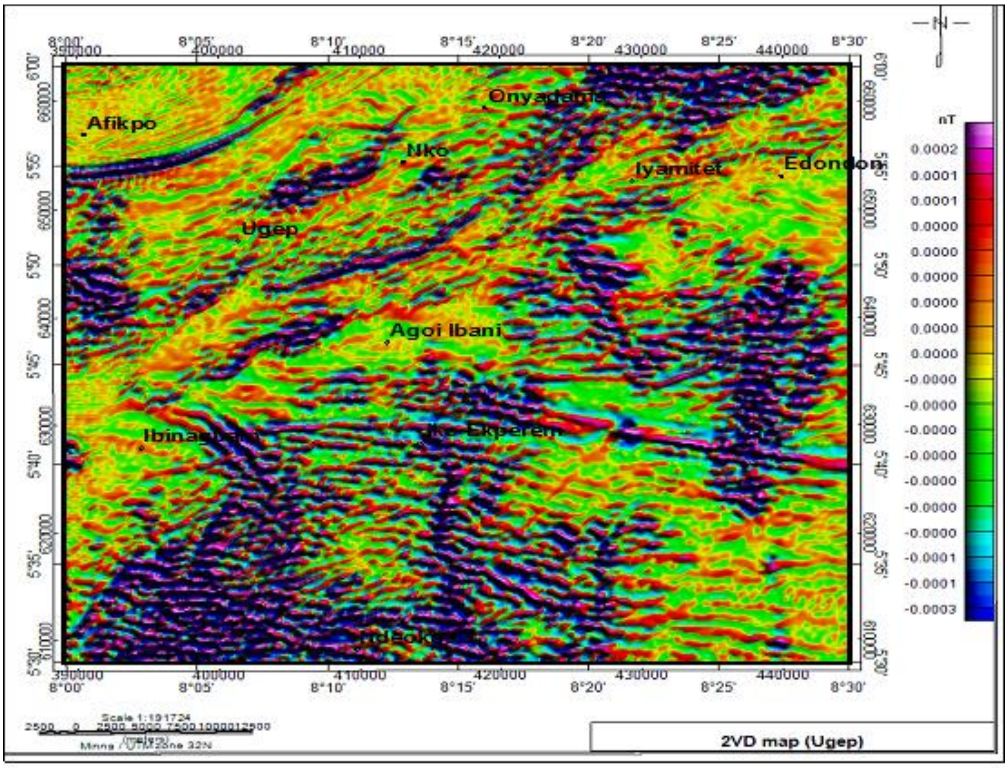

Fig. 9: The second vertical derivatives map of the study area

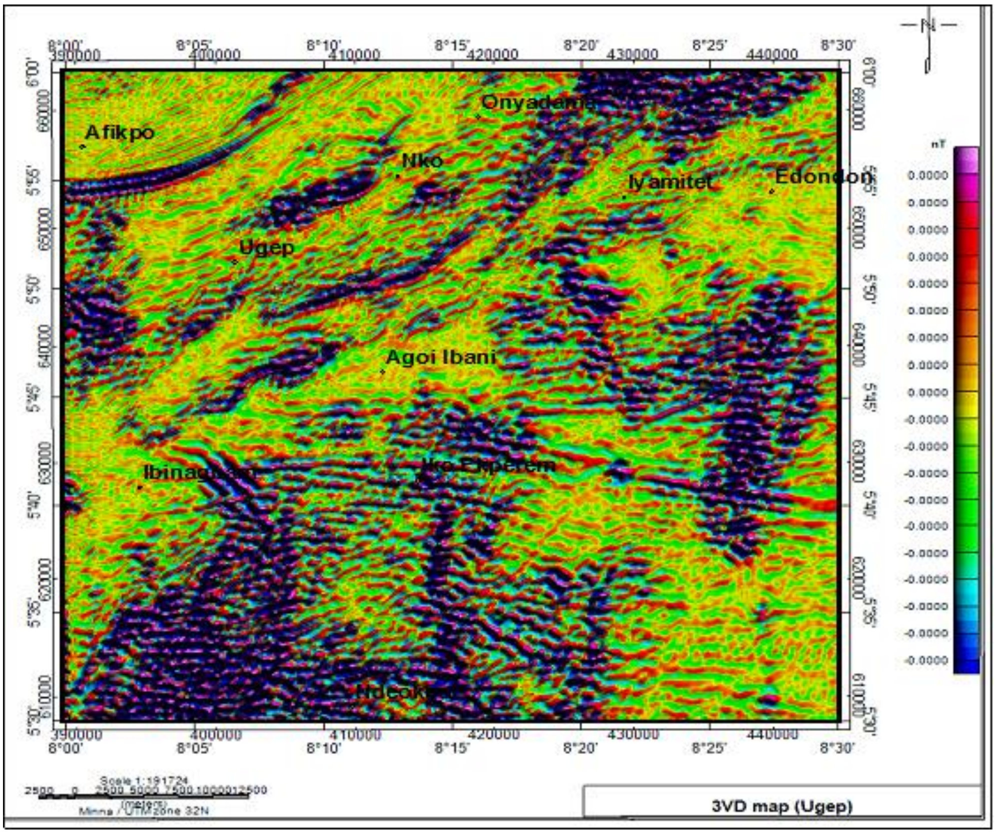

Fig. 10: The third vertical derivative map of the study area

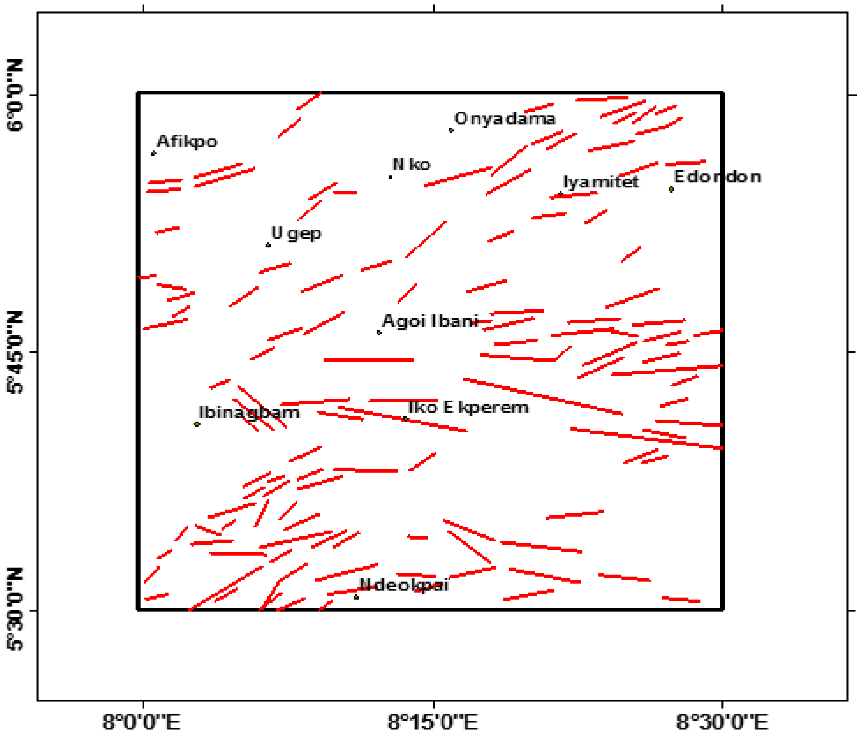

Fig. 11: The lineaments extracted from the second vertical derivative map

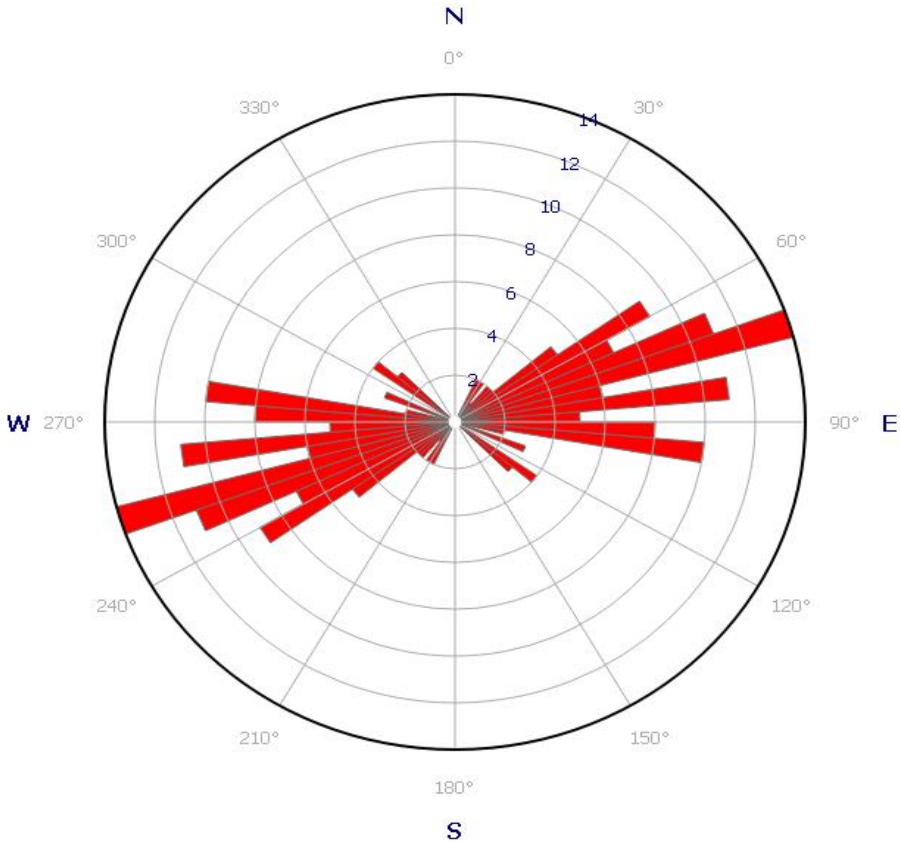

Fig. 12: The Structural Trend analysis on lineament extracted from the second Vertical derivatives map plotted on the Rose diagram

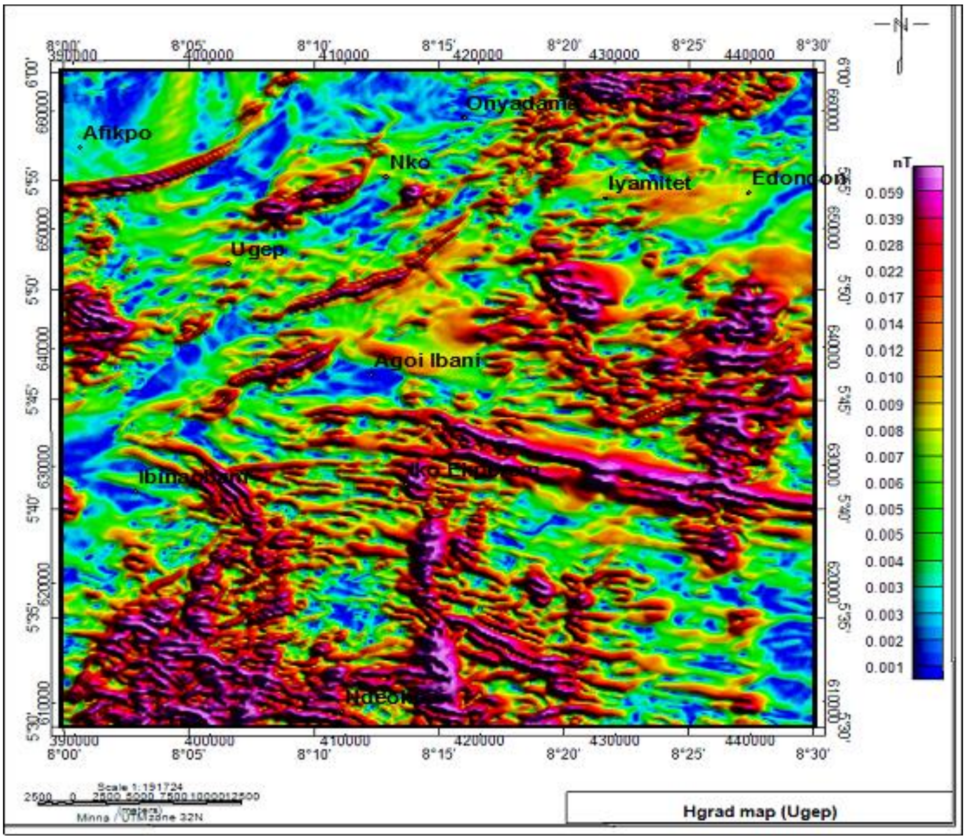

Fig. 13: The horizontal gradient map of the study area

Quantitative interpretation

Analytical signal

Nabighian (1972, 1974) introduced the concept of the analytic signal for magnetic interpretation and showed that its amplitude yields a bell-shaped function over each corner of a 2D body with polygonal cross section. The analytic signal, defined as the anomaly square root of the sum of squares of the horizontal (x and Y) and vertical derivatives (Z) along the orthogonal axes of the anomaly resolves the anomaly maps. Further, the analytical signal of total magnetic intensity (Macleod *et al.*, 2000) is vertically independent of the magnetic inclination of magnetization (Shaung, 1994) and is the better control tool than reduction to pole for interpretation of magnetic anomalies in the middle and low altitudes, and locates the causative bodies more accurately.

The analytical signal shaded image of the study region (Fig. 14) is reflecting similar trends observed in the total magnetic intensity map, which suggests that the magnetic basement occurs at shallow depth or even as outcrop in the study area. Observed closures can in general be attributable to the wide variation in susceptibility of rock-units in zones of fracturing/faulting, the structural orientation of the study area is also seen on the analytical signal map which is consistent with the trend observed on the vertical and the Horizontal derivatives map., with areas in the Southern part having a lot of signals and SW, E and the remaining scattered in other areas on the study area map.

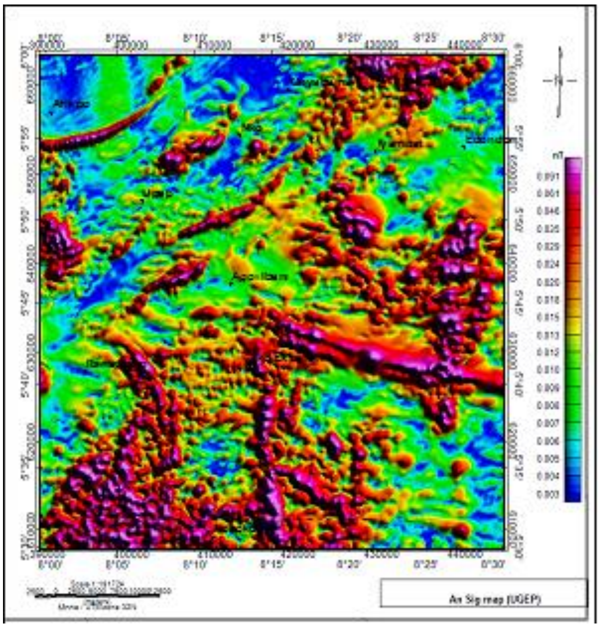

Fig. 14: The color shaded analytical map of Ugep sheet 314

Source parameter imaging (SPI)

The source parameter imaging was used in the depth estimation of the various anomaly sources in the study area; there occurs variation in depth from place to place in the area. The SPI depth (Fig. 10) ranges from -2200 meters to a depth of around -84.0 meters, more than 80 percent of the total area of the map is observed to have a shallow depth values, this is an indication that the depth to the magnetic sources are very shallow and even some areas with depth values lower than -84 m, which is an indication off the basement surface occurring as outcrop with the study area.

These results can be tied to the geologic map of the study areas as shown in Fig. 15, the areas occupied by the basement complex are seen to have a shallow depth while areas that are occupied by the sediments have depth variations this is due to the thin thickness of the sediments in those areas and an indication that the basement in not so far from surface as observed in the Northwestern, and some part of the western part of the study area, some great depth variation are also observed around the North-Eastern part of the study area. The depth values from these depth analyses are consistent with some of the previous work of various authors in the southern Benue basin especially by Oha *et al.* (2016) with depth estimates between 2.5 and 3.5 km.

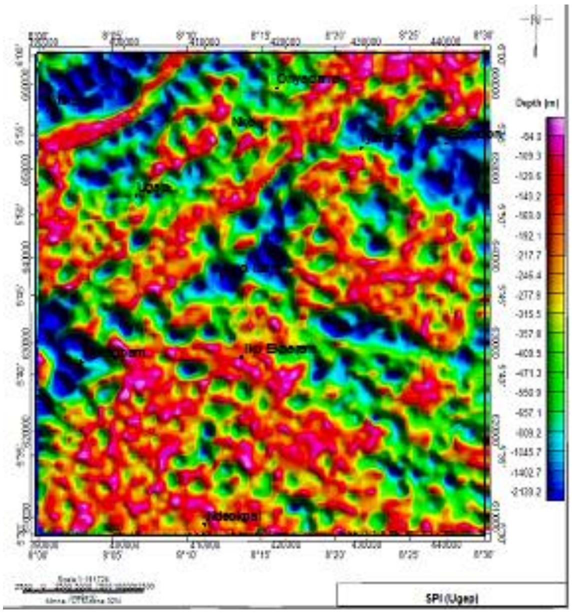

Fig. 15: The color shaded source parameter imaging (SPI) map of the study area

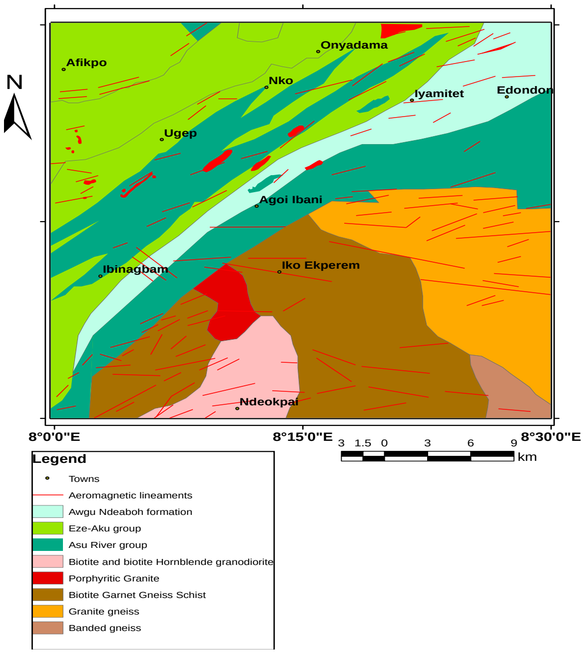

Fig. 16: The Geologic map of the study areas with superimposed lineaments from the second vertical derivatives map used to identify areas with mineralization potential

Litho-structural interpretation

Figure 16 showing the Geologic map of the study area with superimposed lineaments from the Aeromagnetic 2vd map, which can be used as a template for Solid mineral explorations in the study areas as most of the most minerals are structurally controlled especially in Lead/Zinc which has been predominant occurrence in the Southern Benue trough and there has been some known occurrence in the Ishagu area which has the same geological configuration as the Ugep. Areas with likely host of such minerals are the contacts between sedimentary rocks, contacts between basement and sedimentary rocks, areas around the intrusions, areas where the aeromagnetic lineaments coincide with geologic contacts and zones of hydrothermal alterations.

Conclusion

The aeromagnetic data over the Ugep sheet 314 shows a variations in magnetic anomaly from different areas of the map with different anomaly wavelength and different sources as seen from the residual map of the area, the various vertical derivatives, the Horizontal, derivatives and the analytical signals shows a lot of signals coming from a shallow source and most of the sources were being able to be mapped by the third vertical derivatives which is an indication of them being from basement outcrop in most part of the study area.

The structural trends of ENE-SWS, NE-SW, NW-SE trends were observed from the map respectively, the depth to these bodies was determined by the source parameter imaging ranging from -2200 to about -83 meters and it was observed that most of these bodies are from surface outcrop. The area being a sedimentary basin makes us to consider the hydrocarbon prospect, but from our analysis results, we discovered that petroleum prospect in the study areas is very unlikely this is due to a lot of igneous activity in the study area.

Also, the depth of occurrence and the thickness of the sediments is not very favorable for the formation of hydrocarbon and also the sediments' space and accommodation is not very broad, however the prospect in the area should be that of the lead/zinc mineralization which is prominent in the southern Benue trough, these minerals which result from the hydrothermal alteration due to igneous activity should be considered, since these minerals are structurally controlled and there are lot of structures in the areas which are favorable for mineralization.

Recommendation

A more robust data will make us to be able to make a confirmed conclusion on the occurrence of zones of mineral occurrence within the area, I therefore recommend the incorporation of aeroradiometric data to be able to map out zones of alterations within the areas followed by a ground follow up detailed geological mapping, geophysical and geochemical mapping of structures around the identified Alteration zones.

Conflict of Interest

On behalf of all authors, the corresponding author states that there is no conflict of interest, and there was no funding source during this research.

References

Andreasen GE & Zietz I 1969. Magnetic fields for a 4 × 6 prismatic model. US Geological Survey Professional Paper 666.

Baranov V 1957. A new method for interpretation of aeromagnetic maps pseudogravimetric anomalies: *Geophysics*, 22: 359–383.

Baranov V. and Naudy H. 1964. Numerical calculation of the formula of reduction tothe magnetic pole: Geophysics, Vol. 29, pp. 67–79.

Blakely RJ & Simpson RW 1986. Approximating edges of source bodies from magnetic or gravity anomalies. *Geophysics*, 51: 1494-1498.

Davies J, Mushayandebvu MF & Smith R 2004. Magnetic detection and characterization of tertiary and quaternary buried channels. 74th Annual International Meeting, SEG, Expanded Abstracts, p. 734.

Dickson B & Scott K 1997. Interpretation of aerial gamma-ray surveys adding the geochemical factors. AGSO Journal of Australian Geology &Grophysics., 17(2), 187-200.

Gay SP 2004. Glacial till: A troublesome source of near-surface magnetic anomalies: *The Leading Edge*, 23: 542–547.

Grauch VJS, Hudson MR & Minor SA 2001. Aeromagnetic expression of faults that offset basin fill, Albuquerque basin, New Mexico. *Geophysics*, 66: 707-720.

Gunn PJ 1993. Magnetic signatures of gold, copper, Iead-zinc-silver massive sulphide deposits in extensional sedimentary basins. Gunn Geophysics Pty Ltd, 182 pp.

Gunn PJ 1997. Quantitative methods for interpreting aeromagnetic data: A subjective review. *AGSO J. Australian Geology and Geophy.*, 17(2): 105-113.

Hildenbrand TG 1983. FFTFIL--A filtering program based on two-dimensional Fourier analysis: US Geological Survey Open-File Report 83-237, 29 p.

Hildenbrand TG & Raines G 1990. Need for aeromagnetic data and a national airborne geophysics program: US Geological Survey Bulletin 1924, pp. 1–5.

Hsu S, Sibuet JC & Shyu C 1996. High-resolution detection of geologic boundaries from potential field anomalies: an enhanced analytic signal technique. *Geophysics,* 61: 373 - 386.

King LC 1950. Speculations upon the outline and the mode of disruption of Gondwanaland. *Geol. Mag*., 87: 353 -359.

Langenheim VE, Jachens RC, Morton DM, Kistler RW & Matti JC 2004. Geophysical and isotopic mapping of *Preexisting crustal* structures that influenced the location and development of the San Jacinto fault zone, southern California. *Geol. Soc. Am. Bull.*, 116: 1143–1157.

Mendonca CA & Silva JBC 1993. A stable truncated series approximation of the reduction-to-the-pole operator. *Geophysics,* 58: 1084–1090.

Milligan P & Gunn P 1997. Enhancement and presentation of airborne geophysical data. *AGSO J. Australian Geol. & Geophy.*, 17(2): 63-75.

Modisi MP, Atekwana EA, Kampunzu AB & Ngwisanyi TH 2000. Rift kinematics during the incipient stages of continental extension: Evidence from the nascent Okavango rift basin, northwest Botswana. *Geology,* 28: 939–942.

Nabighian MN 1972. The analytic signal of two-dimensional magnetic bodies with polygonal cross-section – Its properties and use for automated anomaly interpretation. *Geophysics,* 37: 507–517.

Obaje NG 2009. Geology and Mineral resources of Nigeria. Springer Dordrecht Heidelbug London New York, pp. 10-30.

Odebode MO 2010. Handout on the Geology of Benue and Anambra Basins, Nigeria.

Oha IA, Onuoha KM, Nwegbu AN & Abba AU. 2016 Interpretation of high resolution aeromagnetic data over southern Benue Trough, southeastern Nigeria. *J. Earth Syst. Sci*., 125(2): 369–385.

Nigerian Geological Survey Agency (NGSA) 2010. Geology and Mineral Resources Map of Nigeria.

Nwajide 2013. Geology of Nigeria’s Sedimentary Basins ISBN 978-978-8401-67-4.

Ojoh KA 1992. The southern part of the Benue Trough (Nigeria) cretaceous stratigraphy, basin analysis, paleo-oceanography and geodynamic evolution in the equatorial domain of the South Atlantic. *NAPE Bull.,* 7: 131–152.

Petters SW 1982. Central West African Cretaceous-Tertiary benthic foraminifera and stratigraphy. *Palaeontographica Abt.* A, 179: 1–104.

Reford MS 1964. Magnetic anomalies over thin sheets. *Geophysics*, 29(4): 532-536.

Reford S, Misener DJ, Ugalde H, Gana J & Oladele O 2012. Paterson, Grant & Watson Limited Nigerian Geological Survey Agency Nigeria’s Nationwide High Resolution Airborne Geophysical Surveys.

Reijers TJA & Nwajide CS 1998. Geology of the Southern Anambra Basin. Unpublished Report for Chevron Nigeria Limited. Field Course Note 66 pp.

Roest W, Verhoef J & Pilkington M 1992. Magnetic Interpretation Using 3-D Analytical Signal.

Roy A 1966. The method of continuation in mining geophysics. *Geoexploration,* 4: 65-83.

Shaung Q 1994. An analytic signal approach to the interpretation of total magnetic anomalies. *Geophysical Prospecting,* 42: 665-675.

Telford WM, Geldart LP & Sheriff RE 1990. Applied Geophysics (Second Edition): Cambridge University Press, 770 p.

Thurston JB & Smith RS 1997. Automatic conversion of magnetic data to depth, dip, and susceptibility contrast using the SPI (TM) method. *Geophysics*, 62(3): 807-813.

Vacquier V, Steenland NC, HendersonRG & Zietz I 1951. Interpretation of Aeromagnetic Maps. Geological Society of America, Memoir 47.